Identification of Contact Residues in the IgE Binding Site of Human FcεRIα†

Justin P. D. Cook,‡ Alistair J. Henry,‡ James M. McDonnell,‡,§ Raymond J. Owens,|| Brian J. Sutton,‡ and Hannah J. Gould*,‡

The Randall Institute, King's College London, 26-29 Drury Lane, London, WC2B 5RL, United Kingdom, and Celltech Therapeutics Ltd., 216 Bath Road, Slough, SL1 4EN, United Kingdom

Received June 2, 1997; Revised Manuscript Received September 3, 1997⊗

ABSTRACT: The high-affinity receptor for immunoglobulin E (IgE), FcεRI, is an $\alpha\beta\gamma_2$ tetramer found on mast cells, basophils, and several other types of immune effector cells. The interaction of IgE with the α-subunit of FcεRI is central to the pathogenesis of allergy. Detailed knowledge of the mode of interaction of FcεRI with IgE may facilitate the development of inhibitors for general use in the treatment of allergic disease. To this end we have performed site-directed mutagenesis on a soluble form of the FcεRI α-chain (sFcεRIα). The effects of four mutations in the second immunoglobulin-like domain of sFcεRIα upon the kinetics of binding to IgE and fragments of IgE have been analyzed using surface plasmon resonance. As described in the preceding paper of this issue [Henry, A. J., et al. (1997) *Biochemistry 36,* 15568−15578], biphasic binding kinetics was observed. Two of the mutations had significant effects on binding: K117D reduced the affinity of sFcεRIα for IgE by a factor of 30, while D159K *increased* the affinity for IgE by a factor of 7, both principally through changes in the rates of dissociation of the slower phase of the interaction. Circular dichroism spectra of sFcεRIα incorporating either of these mutations were indistinguishable from those of wild-type sFcεRIα, demonstrating that the native conformation had not been disrupted. Our results, together with those from site-directed mutagenesis on fragments of IgE presented in the accompanying paper, define the contact surfaces in the IgE:sFcεRIα complex.

Interaction between IgE[1] and its high-affinity receptor, FcεRI, on mast cells and basophils generates receptors for allergen, which can then trigger an allergic response by activation of these cells at sites of allergen challenge (Metzger, 1992; Ravetch & Kinet, 1991; Sutton & Gould, 1993). The products of cell activation initiate an inflammatory cascade in which other cells bearing the receptor, eosinophils and monocytes, participate (Gounni et al., 1994, Maurer et al., 1994), and FcεRI on monocytes has been shown to mediate IgE-dependent allergen presentation (Maurer et al., 1995). Allergens also activate Langerhans cells bearing FcεRI and IgE (Bieber et al., 1992), and these cells migrate to the lymph nodes to maintain T cell memory of the allergen, thus perpetuating hypersensitivity (Wang et al., 1992). We and others are aiming to develop competitive inhibitors of the interaction between IgE and FcεRI, which could be used prophylactically in the treatment of allergy. One of the approaches we have taken is to locate the complementary binding sites in both IgE and the receptor by molecular modeling and mutagenesis.

In the present work, we focus on the receptor FcεRI α-chain, which contains the binding site for IgE (Hakimi et al., 1990; Blank et al., 1991). The extracellular sequence of FcεRIα is predicted to consist of two immunoglobulin-like domains of the C2 type, similar to those found in CD2 and CD4 (McDonnell et al., 1996). It has been shown that a truncated receptor fragment containing only the second, membrane-proximal domain [α(2)] binds to IgE, but with much lower affinity than a soluble fragment of the receptor containing both domains α(1) and α(2) (Robertson, 1993, Scarselli et al., 1993). Production of chimeric receptor α-chains confirmed the principal role of the α(2) domain in IgE binding (Hogarth et al., 1992, Mallamaci et al., 1993). The α(2) domain is predicted to consist of two β-sheets comprising the ABE strands on one face of the domain, and the C′CFG strands on the other. The ABE face contains the three putative *N*-glycosylation sites in α(2). Although the receptor is heterogeneously glycosylated (as deduced from the spread of molecular masses on SDS−PAGE), the molecular mass determined by sedimentation equilibrium indicates that on average all seven putative glycosylation sites are occupied (Keown et al., 1995). Carbohydrate chains are likely to mask the ABE face of α(2), implicating the C′CFG face in binding IgE (Sutton & Gould, 1993). Involvement of the C′CFG face is also consistent with mutagenesis of the homologous subunit of the IgG receptors, FcγRII and FcγRIII (Hogarth et al., 1992; Hulett et al., 1994), and a preliminary report of mutagensis in the α(2) domain of FcεRI (Danho et al., 1995). In addition, we have recently generated an 11-amino acid constrained peptide with the sequence of the C′C strands and intervening loop of α(2), which competes very effectively for IgE binding to the receptor and prevents

† This work was supported by Medical Research Council (U.K.) and National Asthma Campaign (U.K.) project grants to H.J.G. and B.J.S.

* Author to whom correspondence should be addressed: The Randall Institute, King's College London, 26-29 Drury Lane, London, WC2B 5RL, U.K.

‡ The Randall Institute.

§ Present address: Laboratory of Physical Biochemistry, The Rockefeller University, 1230 York Avenue, New York, NY 10021.

|| Celltech Therapeutics Ltd.

⊗ Abstract published in *Advance ACS Abstracts,* November 1, 1997.

[1] Abbreviations: CD, circular dichroism; cDNA, complementary DNA; FBS, foetal bovine serum; IgE, immunoglobulin E; HBS, Hepes buffered saline, pH 7.4; mAb, monoclonal antibody; oligo(dT), oligo deoxythimidine; PBS, phosphate buffered saline, pH 7.4; PCR, polymerase chain reaction; RT-PCR, reverse transcriptase polymerase chain reaction; RU, resonance units; SDS PAGE, sodium dodecyl sulfate−polyacrylamide gel electrophoresis; sFcεRIα, soluble, extracellular region of the α chain of the high-affinity receptor for IgE, FcεRI; SPR, surface plasmon resonance.

S0006-2960(97)01300-7 CCC: $14.00

the sensitization of masts cells by IgE (McDonnell et al., 1996).

In the present work, we have targeted four amino acid residues in α(2) for site-directed mutagenesis. Two of these have a significant effect on IgE binding. One, in the C strand, decreases the affinity for IgE by a factor of 30, while the other, in strand G, *increases* the affinity by a factor of 7. The other two mutations have more subtle effects on the binding kinetics which nevertheless provide additional information about the IgE binding site in α(2) and how this relates to the corresponding site in IgE.

MATERIALS AND METHODS

(a) Cloning the Human FcεRIα cDNA and Construction of the Soluble Fragment. The cDNA encoding the human FcεRIα subunit was obtained by RT-PCR from KU812 cells (ECACC, Porton Down, U.K). Briefly, total RNA was extracted from the cells using the method of Chomczynski and Sacchi (1987). PolyA+ mRNA was prepared by oligo-(dT) affinity chromatography, and first strand cDNA synthesis was carried out by reverse transcriptase. The FcεRIα sequence was then amplified by PCR using the two primers (forward) 5′-GCG CGC AAG CTT CAC AGT AAG CAC CAG GAG TCC-3′ and (reverse) 5′-GCG CGC GAA TTC ATC AGT TGT TTT TGG GGT TTG GC-3′. This full-length PCR product was then subcloned as a *Hin*DIII/*Eco*RI fragment into the psp73 vector (Promega) and sequenced using the chain termination method of Sanger et al. (1977). The truncated cDNA encoding the two extracellular domains [Val1 to Lys176, numbering according to Blank et al. (1989)] was obtained from the full-length cDNA by PCR using the two primers (forward) 5′-GCG CGC AAG CTT CGC CGC CAC CAT GGC TCC TGC CAT GG-3′ and (reverse) 5′-GCG CGC GAA TTC ATC ACT TCT CAC GCG GAG CT-3′. This product was then cloned as a *Hin*DIII/*Eco*RI fragment into the pEE12 expression vector (Bebbington et al., 1992) to give the pEE12/sFcεRIα construct.

(b) Site-Directed Mutagenesis of sFcεRIα cDNA. Circular pEE12/sFcεRIα was used as the template for PCR mutagenesis of the FcεRIa cDNA. This was done using the splice overlap extension method based on that of Ho et al. (1989). This method requires the use of two primers per mutation, one in the sense direction (S) and the other in the antisense direction (A). The sequences of the primers used were, with the mutated sequences underlined: (S) W87D, 5′-TTC AGT GAC GAC CTG CTC CTT-3′; (A) W87D, 5′-AAG GAG CAG GTC GTC ACT GAA-3′; (S) K117D, 5′-GAT GTG TAC GAC GTG ATC TAT-3′; (A) K117D, 5′-ATA GAT CAC GTC GTA CAC ATC-3′, (S) K128D, 5′-GAA GCT CTC GAC TAC TGG TAT-3′, (A) K128D, 5′-ATA CCA GTA GTC GAG AGC TTC-3′, (S) D159K, 5′-TGG CAG CTG AAG TAT GAG TCT-3′; (A) D159K, 5′-AGA CTC ATA CTT CAG CTG CCA-3′. The sequences of the primers used for PCR amplification of the mutated products were 5′ primer, 5′-GCT GAC AGA CTA ACA GAC TGT TCC-3′; 3′ primer, 5′-CAA ATG TGG TAT GGC TGA-3′. PCRs were carried out using Promega *Taq* polymerase in 1x reaction buffer [50 mM KCl, 10 mM tris-HCl, pH 9 at 25 °C, and 0.1% (v/v) Triton X-100], with primers at a concentration of 0.2 mM and in the presence of 0.5% Tween 20 (v/v) and 1.5 mM $MgCl_2$. Reactions contained 0.25 unit of *Taq* polymerase/20 μL of reaction and 1−5 ng of template/reaction. Routinely used cycle conditions were 94 °C for 40 s, 55 °C for 40 s, and 74 °C for 90 s. These conditions were generally used for 15−25 cycles.

*Hin*DIII and *Eco*RI sites in the mutated products facilitated ligation into pEE12. DNA sequences of the subcloned products were checked using chain termination DNA sequencing (Sequenase, USB, Amersham, U.K.).

(c) Transfection and Expression of Wild-Type and Mutant sFcεRIα in NS0 Cells. Prior to selection of transfected colonies, mouse myeloma NS0 cells (ECACC, Porton Down, U.K.) were grown in CB2-DMEM (Gibco BRL) with 10% FBS, 2 mM L-glutamine, 100 units/mL penicillin G sodium, and 100 μg/mL streptomycin sulfate. Cells were incubated at 37 °C with 5% CO_2 and were removed from the tissue culture flasks by sharply tapping the flask sides. After colony selection, NS0 cells were grown in a glutamine free medium, CB2-DMEM with 10% dialyzed FBS, 100 units/mL penicillin G sodium, and 100 μg/mL streptomycin sulfate.

Stable transfections of NS0 cells were carried out by electroporation using a Bio-Rad gene pulser electroporator. For each transfection, 1×10^7 exponentially growing cells were pelleted at 1500 rpm for 5 min. These were then washed twice in ice cold 1× PBS and resuspended in 0.7 mL of ice cold 1× PBS. Linearized pEE12 DNA (40 μg) was then added, typically in a 100 μL volume of a *Sal*I restriction enzyme buffer. The DNA/cell suspension was transferred to a prechilled 0.4 cm electrode gap electroporation cuvette (Bio-Rad) and left on ice for 5 min. The sample was electroporated by two consecutive pulses of 1500 V at 3 μF. The cuvette was then returned to ice for 5 min before the cell suspension was diluted in 140 mL of CB2-DMEM medium including 2 mM L-glutamine, as described above. The cell suspension was then plated into fourteen 96 well plates at 100 μL/well and left overnight at 37 °C. The following day, methionine sulfoxamine was added in a volume of 100 μL/well to give a final concentration of 5 μM. Plates were left for 2−4 weeks to allow selection to take place and selected colonies were then expanded for roller culture.

Cells were seeded at a concentration between 1×10^5 and 1×10^6 in a maximum volume of 250 mL. Cells were split or diluted upon reaching a cell density of 1×10^6 per λ mL. Cells were gassed for 2 min each day with a gas mixture of 5% CO_2, 20% O_2, and 75% N_2. When cell numbers had remained constant for 3 days, the supernatants were harvested by centrifugation at 10 000 rpm (Sorvall RC-2B plus centrifuge, GSA rotor) at 4 °C. Culture supernatants were then passed through a 0.45 μm filter (Millipore) and stored at 4 °C in the presence of 0.1% sodium azide (Sigma).

(d) Purification of Wild-Type and Mutant sFcεRIα Using the 3B4 Anti-FcεRIα mAb. The 3B4 hybridoma produces an anti-FcεRIα α(1) domain monoclonal antibody of the IgG_1 subclass (M. Hogarth, personal communication). The cell line was initially grown in DMEM (Gibco BRL) with 10% FBS, 2 mM L-glutamine, 100 units/mL penicillin G sodium, and 100 μg/mL streptomycin sulfate. The line was then adapted for growth in serum free conditions by a progressive reduction in the amount of FBS, and a corresponding increase in the amount of Hybridoma-SFM medium (Gibco BRL) in the growing cultures. The Hybridoma-SFM was supplemented with 2 mM L-glutamine, 100 units/mL penicillin G sodium, and 100 μg/mL streptomycin sulfate. 3B4 was purified using Protein A sepharose (Sigma), and an anti-

FcεRIα affinity column was made from the purified material by covalently immobilizing it to CNBr-activated sepharose (Pharmacia), according to the manufacturer's instructions.

Harvested sFcεRIα supernatants were circulated over the affinity column overnight at approximately 60 mL/h, and the column was then washed with at least 10 bed volumes of PBS. Bound protein was eluted with 0.2 M glycine, pH 2.5. The eluted protein was neutralized with 1 M Tris and stored ready for further use. Proteins were analyzed by 12% SDS−PAGE (Laemmli, 1970) stained with ISS Pro-Blue (Enprotech, Hyde Park, MA).

(e) CD Analysis of Wild-Type and Mutant sFcεRIα. CD studies were performed on a Jobin-Yvon CD6 spectrophotometer (Longjumeau, France). Wild-type and mutant sFcεRIα samples were analyzed in cylindrical quartz cells of 0.5 mm path length. The spectrophotometer was calibrated for wavelength and ellipticity using *d*-10-camphorsulfonic acid. Measurements were taken at a sample concentration in the range 100−500 μg/mL in 20 mM sodium phosphate buffer, pH 7.4, at constant temperature in a thermostated cell holder.

Spectra were recorded in 0.2 nm steps with an integration time of 4 s and corrected by subtraction of the solvent spectrum obtained under identical conditions. The units of Δε are inverse molarity centimeters per backbone amide.

(f) Preparation of the SPR Sensor Surface. Purified sFcεRIα was coupled to CM5 sensor chips using the aldehyde coupling reaction according to manufacturer's instructions. Briefly, the α-chain was oxidized to introduce aldehyde groups by incubating 100−200 μg of protein with 1 mM sodium metaperiodate (Sigma) on ice for 20 min, in 100 mM sodium acetate buffer, pH 5.5. The sensor chip was then activated using a solution of 50 mM *N*-hydroxysuccinimide (NHS) and 200 mM *N*-ethyl-*N*′-(dimethylaminopropyl)carbodiimide (EDC). Carbohydrazide (5 mM) (Sigma) in 10 mM sodium acetate buffer, pH 4.0, was then injected over the activated surface. This step bound carbohydrazide to the active esters on the chip surface. Any residual esters were inactivated by an injection of 1 M ethanolamine hydrochloride, pH 8.5. The modified sFcεRIα was then injected over the sensor chip until a sufficient quantity had bound. A range of 100−10000 RU was initially tested, and for the data shown in this paper, an immobilization density of 500−1000 RU was used. This low level of immobilized protein is necessary to prevent mass transport effects distorting kinetic measurements. The hydrazone bond formed during aldehyde coupling is unstable at low pH and was thus reduced with 0.1 M sodium cyanoborohydride in 0.1 M acetate buffer, pH 4.0, to enhance its stability. This prevented any loss of the immobilized sFcεRIα during regeneration of the sensor surface with 0.2 M glycine at pH 2.5, which was carried out between experiments to remove all non-covalently bound proteins.

(g) SPR Analysis of Wild-Type and Mutant sFcεRIα. Three proteins were used to probe the interaction with wild-type and mutant sFcεRIα. IgE-WT (Burt et al., 1986) is a myeloma protein, provided by Dr. D. Stanworth and purified as described for IgE-Fc (Young et al., 1995). IgE-Fc, in which the glycosylation sites at Asn265 and Asn371 have been mutated to Gln, has been described in detail elsewhere (Young et al., 1995). Fcε3-4 is a covalently linked dimer consisting of the last two residues of Cε2 and the entire Cε3 and Cε4 domains of IgE. It is secreted from NS0 cells as a dimer due to the presence of the interchain disulfide bond at Cys328 (Shi et al., 1997).

All interactions measured using the BIAcore were carried out at 25 °C, using HBS (BIA certified, being 10 mM Hepes, pH 7.4, 150 mM NaCl, 3.4 mM EDTA, and 0.005% v/v surfactant P-20) as the continuous flow buffer, generally at a flow rate of 10 μL/min. A wide concentration range of analytes (IgE, IgE-Fc and Fcε3-4) was used for the kinetic analyses: 250, 125, 62.5, 31.25, and 15.63 nM, unless otherwise indicated. The analyte was injected for 150 s, followed by HBS for approximately 600 s to monitor the dissociation of bound analyte. The chip was then regenerated with three 60 s pulses of 0.2 M glycine at pH 2.5. The glycine washes had no effect upon the subsequent activity of the chip. Nonspecific binding of the ligand to the sensor surface was assessed by performing sample injections onto a sensor surface which had no protein coupled to it. Under these conditions, there was negligible nonspecific binding for all of the ligands tested.

(h) Kinetic Analysis of SPR Data. Data were analyzed using the BIAevaluation analysis package (version 2.1, Pharmacia Biosensor), as described in the preceding paper in this issue (Henry et al., 1997). Nonspecific binding was subtracted from the specific binding prior to kinetic analysis. Simulations of sensorgrams, using kinetic parameters derived from the kinetic analysis were obtained using BIAsimulation software (version 1.1, Pharmacia Biosensor).

RESULTS

(a) Characterization of Wild-Type and Mutant sFcεRIα. Four mutations were introduced independently into the membrane-proximal α(2) domain of FcεRI: W87D in strand A, K117D in strand C, K128D in strand C′, and D159K in strand G. The first of these is predicted to lie in the linker region between α(1) and α(2) (McDonnell et al., 1996), and mutation of this residue may disrupt any interaction between the domains. The other three mutations involve alteration of the charge on exposed residues on the predicted IgE contact face of α(2) (Sutton & Gould, 1993).

Stable cell lines were generated in NS-0 cells, and recombinant wild-type and mutant sFcεRIα proteins were affinity purified from culture supernatants using the anti-FcεRIα mAb 3B4, which recognizes an epitope in the α(1) domain (Dr. P. M. Hogarth, personal communication). The products were then assessed for purity by SDS−PAGE (Figure 1) and found to exhibit the typical broad bands observed by others for the wild-type fragment and attributed to heterogeneous glycosylation of the α-chain (Blank et al., 1991; Keown et al., 1995; Letourner et al., 1995). Small differences in the mean electrophoretic mobility of the recombinant products (Figure 1) may reflect glycosylation differences that result from variations in the culture conditions (Hayter et al., 1993). The purified proteins were assessed by SPR for immunoreactivity with the anti-FcεRIα mAb 15.1, which recognizes an epitope in the sFcεRI α(2) domain and is inhibitory for IgE binding (Wang et al., 1992). All of the sFcεRIα mutants bound the same amount of mAb 15.1 as wild-type sFcεRIα, implying the maintenance of this epitope (data not shown).

CD spectra were recorded over the range 195−260 nm to assess the secondary structure of the sFcεRIα mutants (Figure 2). sFcεRIα is expected to consist principally of β-sheet

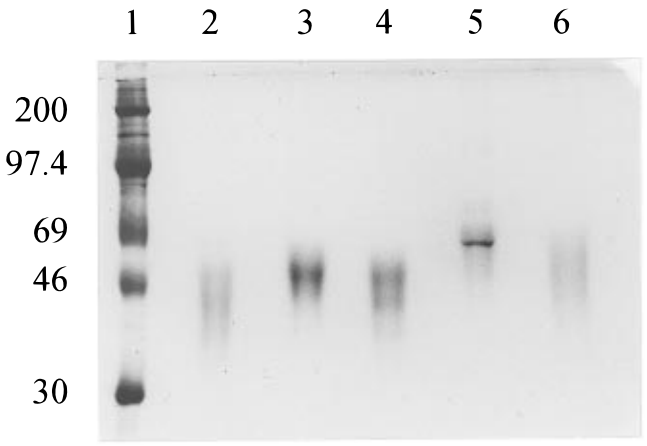

FIGURE 1: SDS−PAGE analysis of purified wild-type and mutant sFcεRIα. Eluates from the 3B4 affinity column were electrophoresed under nonreducing conditions on a 12% SDS−polyacrylamide gel. Lane 1: prestained Rainbow high molecular weight standards (Amersham, U.K.). Lane 2: wild-type sFcεRIα. Lane 3: sFcεRIα(W87D). Lane 4: sFcεRIα(K117D). Lane 5: sFcεRIα-(K128D). Lane 6: sFcεRIα(D159K).

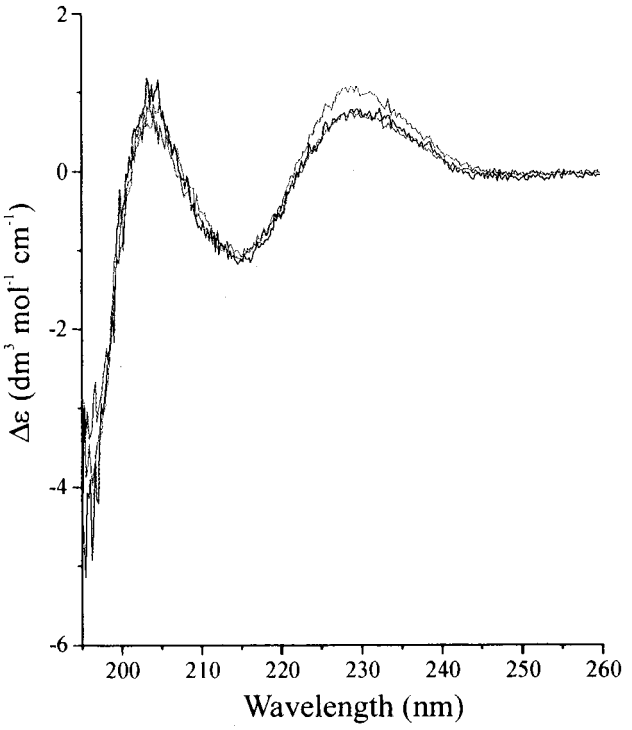

FIGURE 2: Comparison of the CD spectrum of wild-type sFcεRIα with those of sFcεRIα(K117D) and sFcεRIα(D159K). All samples were measured at 400 μg/mL in 20 mM sodium phosphate buffer, pH 7.4, in a 0.5 mm path length cell at 4 °C. Wild-type sFcεRIα, black; sFcεRIα(K117D), red; sFcεRIα (D159K), green.

structure, since it is predicted to comprise two immunoglobulin-like domains (Padlan & Helm, 1992; McDonnell et al., 1996). The positive signal at 203 nm and the negative signal at 215 nm, observed in the spectrum of wild-type sFcεRIα, are indicative of the predicted β-structure, while the positive signal at 230 nm may reflect contributions from the disulfide bonds present in sFcεRIα and also the high density of surface aromatic residues (Kahn, 1979). This spectrum is essentially identical to those published previously (McDonnell et al., 1996; Sechi et al., 1996). The CD spectrum of sFcεRIα(K117D) exhibited a slightly greater ellipticity at 230 nm (Figure 2), but the 215 nm peak and 203 nm trough, which are representative of the β-structure,

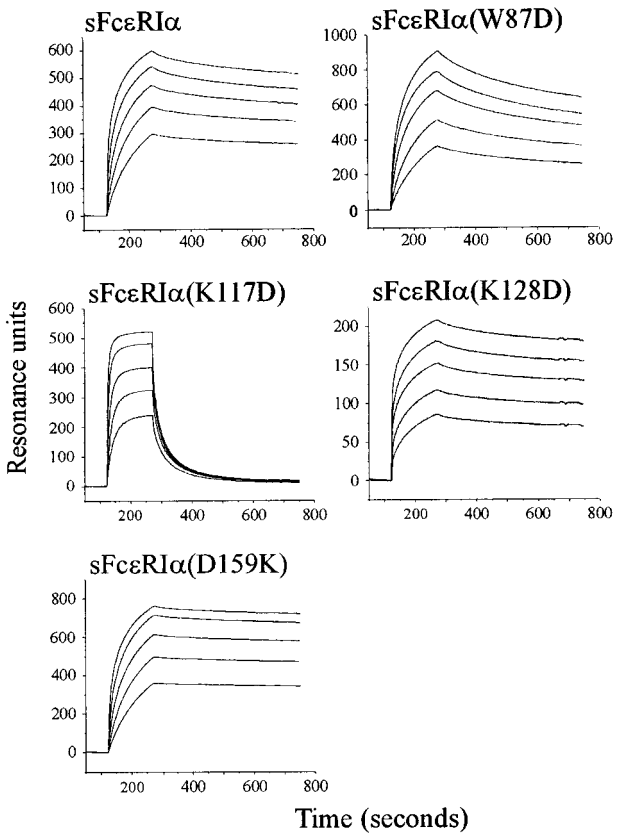

FIGURE 3: Sensorgrams for IgE interacting with wild-type and mutant sFcεRIα. The interactions of wild-type and mutant sFcεRIα with IgE were monitored at five IgE concentrations (250, 125, 62.5, 31.3, and 15.6 nM). A 150 s association phase was followed by a 600 s dissociation phase with HBS buffer flowing over the sensor surface at 10 μL/min. Representative sensorgrams are shown.

are identical to wild-type sFcεRIα. Thermal stability determination by CD indicates that both wild-type sFcεRIα and sFcεRIα(K117D) melt with a single transition at 55 and 60 °C, respectively (data not shown). The fact that the K117D mutation does not change the ellipticity at 215 nm and does not decrease the thermal stability of the protein indicates that the β-structure of sFcεRIα(K117D) has not been disrupted. The spectra of the W89D, K128D (Cook, 1996), and D159K (Figure 2) mutants are identical to wild-type sFcεRIα over the entire recorded spectrum, indicating that these mutations have caused no structural perturbation whatsoever.

(b) Kinetics of Binding of Wild-Type and Mutant sFcεRIα to IgE, IgE-Fc, and Fcε3-4. The kinetics of binding of IgE, IgE-Fc, and Fcε3-4 to immobilized wild-type and mutant sFcεRIα was assessed by SPR. Figure 3 shows sensorgrams for the interaction of IgE with the wild-type and mutant receptors. It may be seen that there is a large difference between the sensorgrams for wild-type sFcεRIα and sFcεRIα-(K117D). Not only is there a lower response (reflected in the number of RUs recorded), but the off-rate is clearly much faster for this mutant than for wild-type sFcεRIα. It can also be seen that the dissociation of IgE from sFcεRIα-(D159K) is slower than that from wild-type sFcεRIα. These trends persist in the sensorgrams for the interactions of IgE-Fc and Fcε3-4 with the wild-type and mutant sFcεRIα (data not shown).

Initial fitting of data was carried out using monophasic models of association and dissociation. However, it was

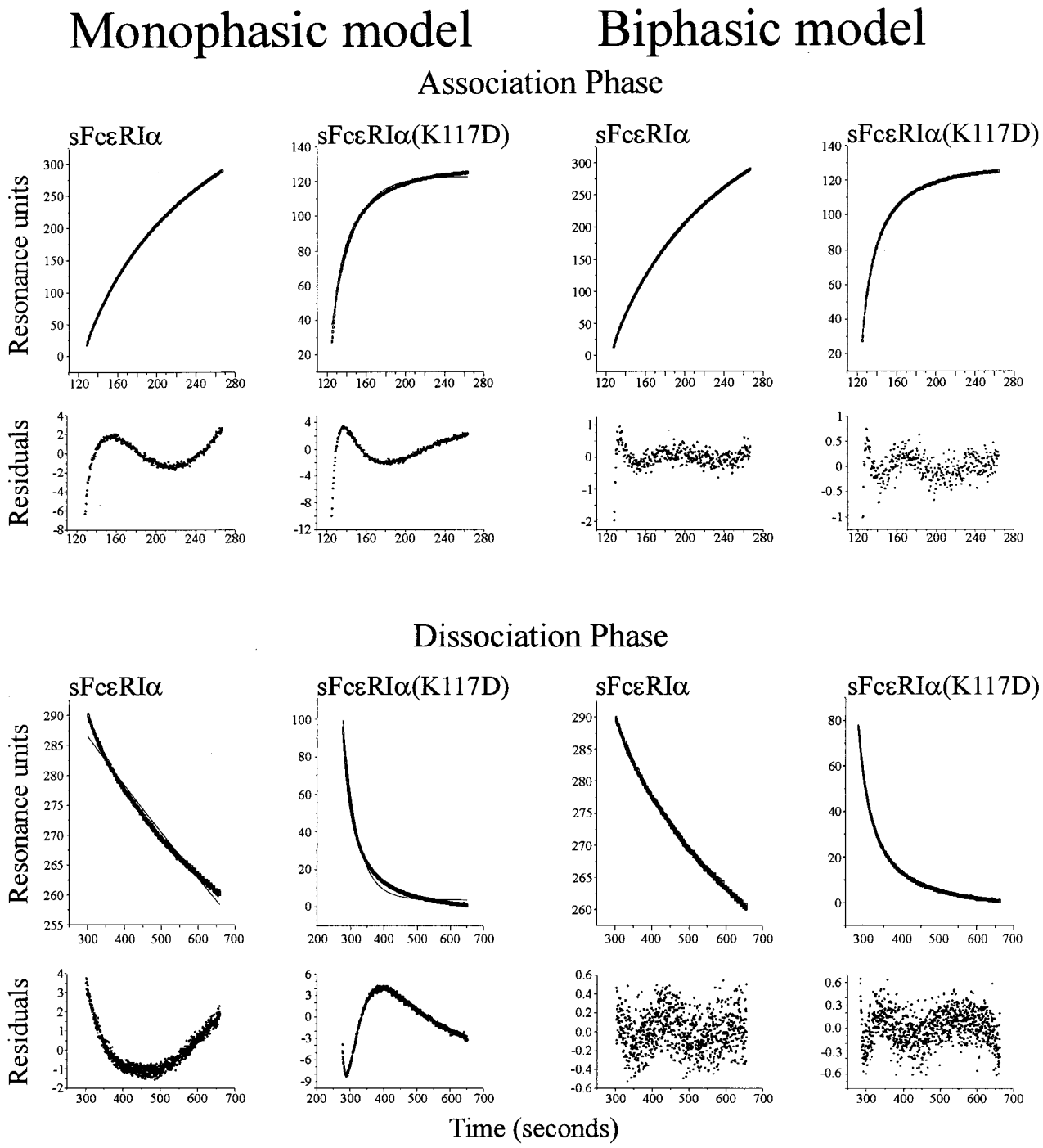

FIGURE 4: Analysis of SPR data for IgE binding to immobilized wild-type sFcεRIα or sFcεRIα(K117D). The association and dissociation phases of the interaction were fitted to monophasic and biphasic models of binding. The fitted lines are overlaid with the experimental data curves in each plot. The residual plots (obtained by subtracting the calculated fit from the experimental data) are shown for each fit. Analysis of wild-type and mutant sFcεRIα is illustrated here for the curves corresponding to 250 nM IgE.

clear that the data could not be satisfactorily described by a simple monophasic model, while an excellent fit was obtained with biphasic models of association and dissociation. This can be seen in Figure 4, which shows the data analysis for the interaction of IgE with wild-type sFcεRIα and sFcεRIα(K117D). The residual values for the monophasic fits are very high- and nonrandomly distributed along the curve, whereas those for the biphasic fits are considerably smaller and are randomly distributed. Similarly, the binding data for IgE and Fc fragments with all of the mutants were best fitted by a biphasic model.

The biphasic fits are characterized by two association rates and two dissociation rates, and these values yield an affinity constant for each phase of the interaction (Table 1). These may be characterized as a fast, lower affinity, and a slow, higher affinity interaction. The K_{a2} value for the latter interaction of 2.7×10^9 M^{-1} for IgE binding to wild-type sFcεRIα is slightly lower than the values obtained from cell binding assays, which are on the order of 10^{10} M^{-1} (Hakimi et al., 1990; Basu et al., 1993; Mallamaci et al., 1993; Young et al., 1995; Keown et al., 1997). The K_{a2} values determined for IgE-Fc and Fcε3-4 are on the same order as those for IgE, namely, 3.3×10^9 and 1.5×10^9 M^{-1}, respectively.

IgE exhibits a 30-fold lower affinity for sFcεRIα(K117D) and a 7-fold *higher* affinity for sFcεRIα(D159K) than for wild-type sFcεRIα (K_{a2} values, Table 1). The dramatic effect

Table 1: Summary of the Kinetic Data for the Interactions of Wild-Type and Mutant sFcεRIα Proteins with IgE, IgE-Fc, and Fcε3-4, as Determined by Surface Plasmon Resonance[a]

protein assayed	k_{a1} (M^{-1} s^{-1})	k_{a2} (M^{-1} s^{-1})	k_{d1} (s^{-1})	k_{d2} (s^{-1})	K_{a1} (M^{-1})[b]	K_{a2} (M^{-1})[a]	R_1/R_0
Constants for Interaction with IgE-WT							
wt FcεRIα	$(3.5 \pm 0.9) \times 10^5$	$(8.6 \pm 3.5) \times 10^4$	$(1.2 \pm 0.1) \times 10^{-2}$	$(3.2 \pm 0.8) \times 10^{-5}$	2.9×10^7	2.7×10^9	0.06
W87D	$(8.6 \pm 7.7) \times 10^5$	$(1.5 \pm 1.2) \times 10^5$	$(9.2 \pm 0.8) \times 10^{-3}$	$(3.9 \pm 0.1) \times 10^{-4}$	9.3×10^7	3.9×10^8	0.13
K117D	$(1.3 \pm 0.6) \times 10^6$	$(4.6 \pm 3.7) \times 10^5$	$(3.8 \pm 0.5) \times 10^{-2}$	$(4.6 \pm 1.1) \times 10^{-3}$	3.4×10^7	9.9×10^7	0.74
K128D	$(6.9 \pm 2.9) \times 10^5$	$(1.6 \pm 1.1) \times 10^5$	$(1.3 \pm 0.1) \times 10^{-2}$	$(3.4 \pm 0.6) \times 10^{-5}$	5.3×10^7	4.6×10^9	0.11
D159K	$(4.4 \pm 1.6) \times 10^5$	$(1.2 \pm 0.6) \times 10^5$	$(1.4 \pm 0.1) \times 10^{-2}$	$(6.3 \pm 0.9) \times 10^{-6}$	3.2×10^7	1.9×10^{10}	0.01
Constants for Interaction with IgE-Fc							
wt FcεRIα	$(1.6 \pm 0.7) \times 10^6$	$(2.5 \pm 1.8) \times 10^5$	$(9.4 \pm 0.8) \times 10^{-3}$	$(7.5 \pm 1.5) \times 10^{-5}$	1.7×10^8	3.3×10^9	0.06
W87D	$(1.0 \pm 0.4) \times 10^6$	$(2.1 \pm 1.3) \times 10^5$	$(8.8 \pm 0.1) \times 10^{-3}$	$(4.0 \pm 0.1) \times 10^{-4}$	1.1×10^8	5.3×10^8	0.15
K117D	$(1.8 \pm 0.3) \times 10^6$	$(6.4 \pm 4.4) \times 10^5$	$(2.8 \pm 2.0) \times 10^{-2}$	$(2.0 \pm 0.2) \times 10^{-3}$	6.3×10^7	3.2×10^8	0.73
K128D	$(3.8 \pm 1.6) \times 10^6$	$(2.9 \pm 2.2) \times 10^5$	$(1.2 \pm 0.9) \times 10^{-2}$	$(6.6 \pm 1.6) \times 10^{-5}$	3.3×10^8	4.5×10^9	0.05
D159K	$(1.1 \pm 0.2) \times 10^6$	$(1.9 \pm 1.1) \times 10^5$	$(1.1 \pm 0.7) \times 10^{-2}$	$(1.0 \pm 0.2) \times 10^{-5}$	1.0×10^8	1.9×10^{10}	0.02
Constants for Interaction with Fcε3-4							
wt FcεRIα	$(1.1 \pm 0.5) \times 10^6$	$(9.6 \pm 3.9) \times 10^5$	$(1.6 \pm 0.2) \times 10^{-2}$	$(6.3 \pm 0.8) \times 10^{-4}$	7.2×10^7	1.5×10^9	0.18
W87D	$(1.1 \pm 0.5) \times 10^6$	$(9.5 \pm 2.6) \times 10^5$	$(2.0 \pm 0.2) \times 10^{-2}$	$(3.6 \pm 0.2) \times 10^{-3}$	5.6×10^7	2.6×10^8	0.52
K117D	$(5.6 \pm 0.8) \times 10^6$	$(6.3 \pm 4.9) \times 10^5$	$(1.5 \pm 0.1) \times 10^{-1}$	$(1.2 \pm 0.4) \times 10^{-3}$	3.7×10^7	5.3×10^8	0.52
K128D	$(4.8 \pm 0.3) \times 10^5$	$(1.5 \pm 1.4) \times 10^5$	$(1.2 \pm 0.2) \times 10^{-2}$	$(7.0 \pm 0.3) \times 10^{-4}$	3.9×10^7	2.1×10^8	0.18
D159K	$(1.4 \pm 0.5) \times 10^5$	$(1.9 \pm 0.1) \times 10^6$	$(1.4 \pm 0.1) \times 10^{-2}$	$(4.5 \pm 0.4) \times 10^{-4}$	1.0×10^7	4.4×10^9	0.10

[a] Sensorgrams were analyzed using a biphasic model for the interaction. Results are expressed as mean ± sd for five separate determinations. [b] Calculated as k_{a1}/k_{d1}. [c] Calculated as k_{a2}/k_{d2}.

on the affinity of IgE for sFcεRIα(K117D) is due principally to a 145-fold increase in the dissociation rate of the second component of the interaction, ($k_{d2} = 4.6 \times 10^{-3}$ s^{-1}, compared with 3.2×10^{-5} s^{-1} for wild-type sFcεRIα). Similarly, the 7-fold *increase* in the affinity of IgE for sFcεRIα(D159K) is due principally to a 5-fold decrease in the dissociation rate k_{d2} relative to wild-type sFcεRIα (6.3×10^{-6} and 3.2×10^{-5} s^{-1}, respectively). The kinetic parameters of the two remaining mutants, sFcεRIα(W87D) and sFcεRIα(K128D), are also described in Table 1. sFcεRIα(K128D) is indistinguishable from wild-type sFcεRIα, but sFcεRIα(W87D) displays a modest decrease in the affinity of the second component (K_{a2}), due to a 12-fold increase in the dissociation rate k_{d2} (3.9×10^{-4} s^{-1}, compared with 3.2×10^{-5} s^{-1} for wild-type).

The K117D mutation also has a dramatic effect on the ratio of the two components of the biphasic interaction, which can be estimated from the kinetic analysis. The parameter R_0 represents the total binding signal at equilibrium, while R_1 is the binding due to the fast, lower affinity phase; thus, the ratio R_1/R_0 (Table 1) is the fractional contribution of the fast, lower affinity, phase. These values indicate that for the interaction between wild-type sFcεRIα and wild-type IgE, the slow, higher affinity phase dominates overwhelmingly at 94% of total binding. However, the K117D mutation alters the ratio such that only 26% of total binding is contributed by the slow, higher affinity phase, and for this mutant, the fast, lower affinity phase predominates. This reversal of the relative contribution of the fast and slow phases to the overall binding is illustrated in the simulated curves shown in Figure 5, which are based upon the experimentally derived kinetic parameters. These curves are discussed further below.

(c) Kinetics of Binding of Wild-Type and Mutant sFcεRIα to IgE-Fc(R334S). IgE-Fc(R334S) is a mutant of IgE-Fc in which Arg334, at the N-terminal end of strand A in Cε3, has been substituted by serine. This mutation greatly increases the rate of dissociation of IgE-Fc from membrane-bound or immobilized sFcεRIα, resulting in a 120-fold decrease in the affinity for the receptor (Henry et al., 1997). The kinetics of binding of IgE-Fc(R334S) to wild-type

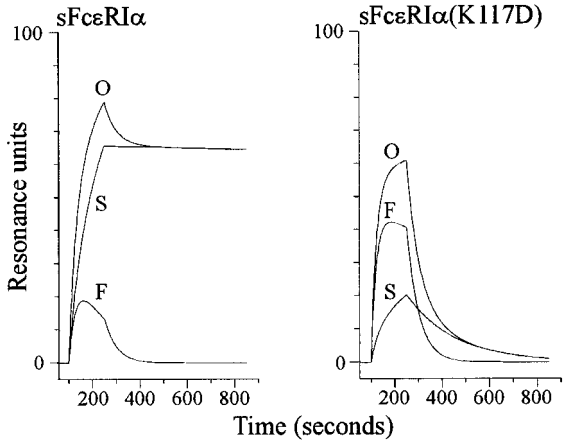

FIGURE 5: Simulated sensorgrams for IgE binding to wild-type sFcεRIα and sFcεRIα(K117D). The contribution of the two components of the biphasic interaction to the observed SPR response was modeled using kinetic parameters obtained from the biphasic fitting of the SPR data. Injection times were modeled to be identical to those of the experimental method. F, contribution from the fast, low-affinity component; S, contribution of the slow, high-affinity component; O, the observed SPR response.

sFcεRIα and the four mutants were examined (Figure 6). The binding activity of IgE-Fc(R334S) to wild-type sFcεRIα is significantly diminished relative to that of wild-type IgE-Fc, ($K_{a2} = 1.0 \times 10^7$ M^{-1}, Table 2 compared with 3.3×10^9 M^{-1} for wild-type IgE-Fc, Table 1) as previously observed (Henry et al., 1997, Figure 3). The binding of IgE-Fc(R334S) to sFcεRIα(K117D), however, is barely detectable (Figure 6; note scale of RU axis), and too low for any kinetic parameters to be determined. The fact that the binding affinity between these two mutant species is less than that measured for either mutation alone indicates that the two contact residues, Arg334 in IgE-Fc and Lys117 in sFcεRIα, must contribute independently to the interaction.

The K128D mutation has no effect upon the binding of wild-type IgE-Fc ($K_{a2} = 4.5 \times 10^9$ M^{-1}, Table 1), but the affinity of IgE-Fc(R334S) is significantly diminished ($K_{a2} = 2.4 \times 10^6$ M^{-1} compared with 1.0×10^7 M^{-1}, Table 2). The W87D mutation has a modest effect on the binding of wild-type IgE-Fc, which is increased in IgE-Fc(R334S). The

Table 2: Summary of the Kinetic Data for the Interaction of Wild-Type and Mutant sFcεRIα Proteins with IgE-Fc(R334S), as Determined by Surface Plasmon Resonance[a]

protein assayed	k_{a1} (M^{-1} s^{-1})	k_{a2} (M^{-1} s^{-1})	k_{d1} (s^{-1})	k_{d2} (s^{-1})	K_{a1} (M^{-1})[b]	K_{a2} (M^{-1})[c]	R_1/R_0
			Constants for Interaction with IgE-Fc(R334S)				
wt FcεRIα	$(1.3 \pm 1.1) \times 10^5$	$(3.2 \pm 2.9) \times 10^4$	$(2.9 \pm 0.3) \times 10^{-2}$	$(3.1 \pm 0.3) \times 10^{-3}$	4.5×10^6	1.0×10^7	0.62
K128D	$(2.2 \pm 0.9) \times 10^5$	$(1.6 \pm 0.9) \times 10^4$	$(7.2 \pm 1.7) \times 10^{-2}$	$(6.7 \pm 1.3) \times 10^{-3}$	3.0×10^6	2.4×10^6	0.49
D159K	$(2.4 \pm 1.8) \times 10^4$	$(9.8 \pm 6.9) \times 10^4$	$(1.8 \pm 0.2) \times 10^{-2}$	$(3.1 \pm 0.5) \times 10^{-3}$	1.3×10^6	3.2×10^7	0.56

[a] Sensorgrams were analyzed using a biphasic model for the interaction. Results are expressed as mean ± sd for five separate determinations. [b] Calculated as k_{a1}/k_{d1}. [c] Calculated as k_{a2}/k_{d2}.

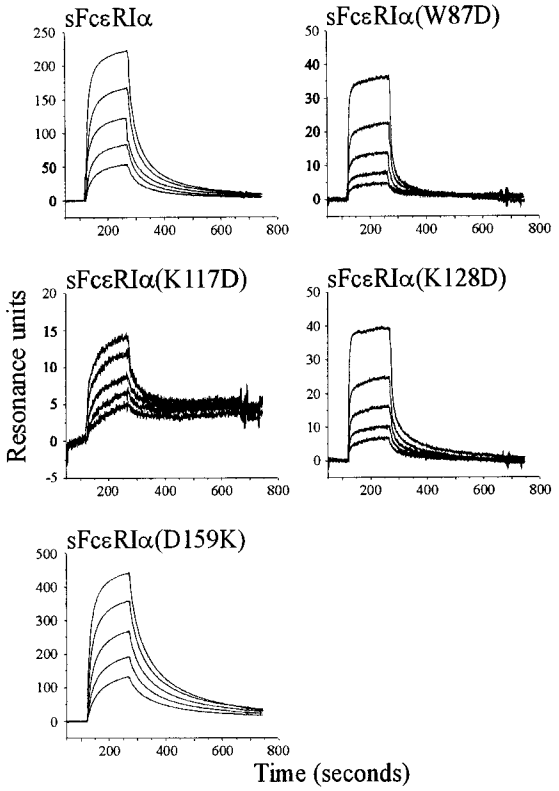

FIGURE 6: Sensorgram of IgE-Fc(R334S) interacting with wild-type and mutant sFcεRIα. The interactions of wild-type and mutant sFcεRIα with IgE-Fc(R334S) were monitored as described in Figure 2, except for the use of higher concentrations for the interaction of sFcεRIα(K117D) with IgE-Fc(R334) where the doubling dilution concentration series was started at a concentration of 5 mM.

D159K mutation, however, which *enhances* the binding of wild-type IgE-Fc ($K_{a2} = 1.9 \times 10^{10}$ M^{-1} compared with 3.3×10^9 M^{-1} for wild-type sFcεRIα, Table 1), appears also to enhance the binding of IgE-Fc(R334S) to a similar extent ($K_{a2} = 3.2 \times 10^7$ M^{-1} compared with 1.0×10^7 M^{-1} for wild-type sFcεRIα, Table 2).

DISCUSSION

Our results build upon previous studies of the FcεRI α-chain, which show that the IgE binding site lies principally within the membrane-proximal, extracellular α(2) domain (Robertson, 1993; Scarselli et al., 1993, Mallamaci et al., 1993). Several lines of indirect evidence had earlier pointed to the involvement of the four-stranded C′CFG face of this domain [reviewed in Sutton and Gould (1993)], and this has recently been confirmed by a preliminary report of mutagenesis within this region (Danho et al., 1995) and studies of a constrained peptide with inhibitory activity corresponding to the C′C strands and intervening loop region (McDonnell et al., 1996).

We chose to work with soluble fragments of the receptor for two reasons. Firstly, we could assess the effects of the mutations on the conformation of sFcεRIα by CD spectroscopy, which would not have been possible with the membrane-bound form. None of the mutations appeared to cause any structural perturbations (Figure 2). Secondly, we could study the binding of IgE, IgE-Fc, and Fcε3-4 to sFcεRIα by surface plasmon resonance. This technique allows the association and dissociation kinetics to be determined in real time without labeling of either component (which can lead to a degree of inactivation of the labeled material). When studying the effects of individual amino acid residue substitutions, it is important to be able to determine the effects upon both association and dissociation events, as affinity measurements alone may not reflect any changes in the kinetics of interaction.

The present work extends our knowledge of the binding site by identifying amino acid residues in FcεRIα that either make contact with IgE or are in close proximity to the binding site. Four mutations were chosen: K117D in strand C, K128D in strand C′, D159K in strand G, and W87D in the N-terminal linker region of the α(2) domain (strand A). Our results show that Lys117 must be a contact residue, since substitution by aspartic acid results in a 30-fold reduction in binding affinity for IgE (and for the IgE-Fc fragments). In contrast, the effect of substituting Asp159 by lysine causes an *increase* in the affinity for IgE by a factor of 7. Not only does this imply that Asp159 must be close to or part of the site, but it demonstrates that the high affinity of the IgE-FcεRI interaction can be further enhanced. Lys128 on the other hand, when substituted by aspartic acid, has no detectable effect upon the binding of wild-type IgE or IgE-Fc, but when the latter incorporates the mutation R334S, a dramatic reduction in binding is observed (Figure 6). This implies that Lys128 must at least be in close proximity to the site. Finally, substitution of Trp87 by aspartic acid, in the N-terminal linker region and partially buried in the model of the α(2) domain (McDonnell et al., 1996), causes only a modest effect that may be due to alterations in the relative disposition of the two domains. Like the K128D mutation however, the W87D mutation causes a much more substantial effect upon the interaction with IgE-Fc(R334S).

We have extensively investigated the interaction between IgE, IgE-Fc, Fcε3-4, and site-specific mutants thereof, with wild-type sFcεRIα, by SPR (Henry et al., 1997). These studies demonstrated that the interaction could not be described by a simple monophasic model of binding, but consisted of two components, a fast, lower affinity phase and a slow, higher affinity phase. The experiments reported in the preceding paper in this issue (Henry et al., 1997) show that the biphasicity observed in SPR is not due to sample heterogeneity, artefacts of immobilization, or distortion of

the kinetics by mass transport effects (Edwards et al., 1995). In the studies presented in the present paper, gluteraldehyde coupling was used when comparing the receptor mutants as the mutagenesis altered the number of lysines available of amine coupling. The wild-type receptor was immobilized by gluteraldehyde or amine coupling to the sensor surface, with no difference in the kinetics of IgE or IgE-Fc binding (data not shown). While it may have been preferable to immobilize the IgE and fragments for analysis of the sFcϵRIα mutants, this could not be achieved despite extensive attempts involving different immobilization chemistries (coupling by primary amines, carbohydrate, cysteine substitution, and biotinylation) and different sources of IgE. However, immobilization of the sFcϵRIα mutants as described here, enabled direct comparison to be made with the results for immobilized wild-type receptor (Henry et al., 1997).

The two affinity constants which characterize the interaction between wild-type sFcϵRIα and IgE are 2.9×10^7 M^{-1} for the faster phase and 2.7×10^9 M^{-1} for the slower phase (Table 1). A simulation of the contributions of each component to the overall observed binding curves is shown in Figure 5. In the very early stages of binding, the fast, lower affinity component predominates, but at later times the slow, higher affinity component takes over; we have observed experimentally that the fractional use of the latter component does indeed increase as the association time is increased (data not shown). This explains why the interaction has generally been considered to be monophasic, since in the past either equilibrium-based methods (Mallamaci et al., 1993) or kinetic methods (Hakimi et al., 1990; Kulczycki & Metzger, 1974; Mallamaci et al., 1993; Riske et al., 1991; Young et al., 1995) which do not permit the rapid sampling necessary to detect the fast phase, have been used. The affinity constant for the high-affinity phase determined by SPR, however, is still slightly lower than the values of the order of 10^{10} M^{-1} obtained in previous studies with cell binding assays. Both FcϵRIα and FcγRIα are associated with a γ-chain dimer in the cell membrane (Ravetch & Kinet, 1991), and recent work on the IgG/FcγRI interaction revealed a contribution from the γ-chains to the affinity of the receptor complex for the ligand in the context of the cell membrane (Miller et al., 1996). The lower affinity of IgE for isolated sFcϵRIα, as observed by SPR, may be due to the absence of the γ-chains.

The K117D mutation may be seen to have an even more dramatic effect when the individual on- and off-rates of the two components of the biphasic interaction are considered. The off-rate for the slow, higher affinity phase, k_{d2}, is enhanced 145-fold (Table 1), while the rates for the faster phase are virtually unchanged. Also affected however is the ratio of the two components (represented by the ratio R_1/R_0 in Table 1), calculated from the predicted maximum RU values at equilibrium for each component. Thus while IgE binding to wild-type sFcϵRIα comprises 6% of the fast, lower affinity phase and 94% of the slow, higher afffinity phase, for the K117D mutant the balance is reversed so that the fast phase contributes 74%, the slow phase 26%. This is clearly illustrated in the simulation shown in Figure 5b. This shift in the fractional contributions of the two phases by a mutation in the immobilized component is further evidence that the biphasicity is not an artefact of the immobilization or a mass transport effect. The principal conclusion therefore is that Lys117 contributes to the slow, higher affinity phase of the interaction. In a similar way, the effect of the D159K mutation, which increases the affinity of the interaction compared to wild-type sFcϵRIα, is largely the result of a 5-fold decrease in the k_{d2} value. This implies that Asp159 also is more involved in the slow, higher affinity phase of the interaction, and leads to tighter binding than with the native lysine residue.

The results of studying the effects of mutations in sFcϵRIα upon the binding of IgE-Fc carrying the R334S mutation provides further information about the complex. This mutation in IgE-Fc dramatically reduces the binding affinity, again in the slow, higher affinity phase (Henry et al., 1997). However, the fact that the K117D mutation in sFcϵRIα reduces binding further, to an almost undetectable level, shows that the two residues Lys117 and Arg334 must contribute independently to the interaction. Similarly, the fact that the K128D mutation further decreases the binding of IgE-Fc(R334S) indicates that these two residues also contribute independently.

The data presented in the preceding paper in this issue (Henry et al., 1997), together with the work of Presta et al. (1994), allow predictions to be made about the binding site for FcϵRIα in IgE-Fc. Presta et al. (1994) carried out an exhaustive study of 67 point and homologue scanning mutations in the IgE-Fc, and Figure 7a shows the location of these mutations, both those which affected binding (orange), and those that did not (green), in the predicted structure of the IgE-Fc (Padlan & Davies, 1986; Helm et al., 1991). Superimposed on this figure (in red) are the mutations P333Q (Beavil et al., 1993) and R334S (Henry et al., 1997), which also affect binding. It is clear that residues indicated in red and orange form a contiguous region that extends over both Ce3 domains on one side of the IgE-Fc, and the locations of the residues found to have no effect on IgE binding (indicated in green) serve to define its boundaries. Furthermore, the distance between the two extremities of this site is approximately 3.8 nm, whereas the maximum dimension across the C′CFG binding face of the FcϵRI α(2) domain is at most 3.0 nm. Thus, the extent of the IgE-Fc binding region implies the involvement of both sFcϵRIα domains.

The results presented in this paper identify Lys117 as a contact residue and both Lys128 and Asp159 as being near to the IgE binding site in FcϵRI α-chain. Two of these mutations, Lys117 and Asp159, are shown in red in the predicted structure of sFcϵRIα in Figure 7b. The peptide Ile119-Tyr129, which has been shown to inhibit IgE binding to sFcϵRIα (McDonnell et al., 1996), is identified in yellow in Figure 7b. Residue Lys128 lies within this sequence. Superimposed on this structure are the results of Danho et al. (1995) and Mallamaci et al. (1993). The former authors identified 12 residues in α(2) to be important for IgE-binding (Val115, Lys117, Val118, Tyr120, Tyr121, Lys122, Asp123, Tyr129, Tyr131, Tyr149, Gly153, and Val 155, shown in orange). Mallamaci et al. (1993) identified regions in the α(1) domain that are not involved in binding IgE (indicated in green in Figure 7b). All of the regions highlighted by Mallamaci et al. are distal from α(2) in the predicted structure of the α-chain, and thus the loops proximal to the α(2) domain may be involved in IgE-binding. Comparison between panels a and b of Figure 7 reveals that the two binding regions are of similar extent, but in order to build a plausible model of the complex, further complementation

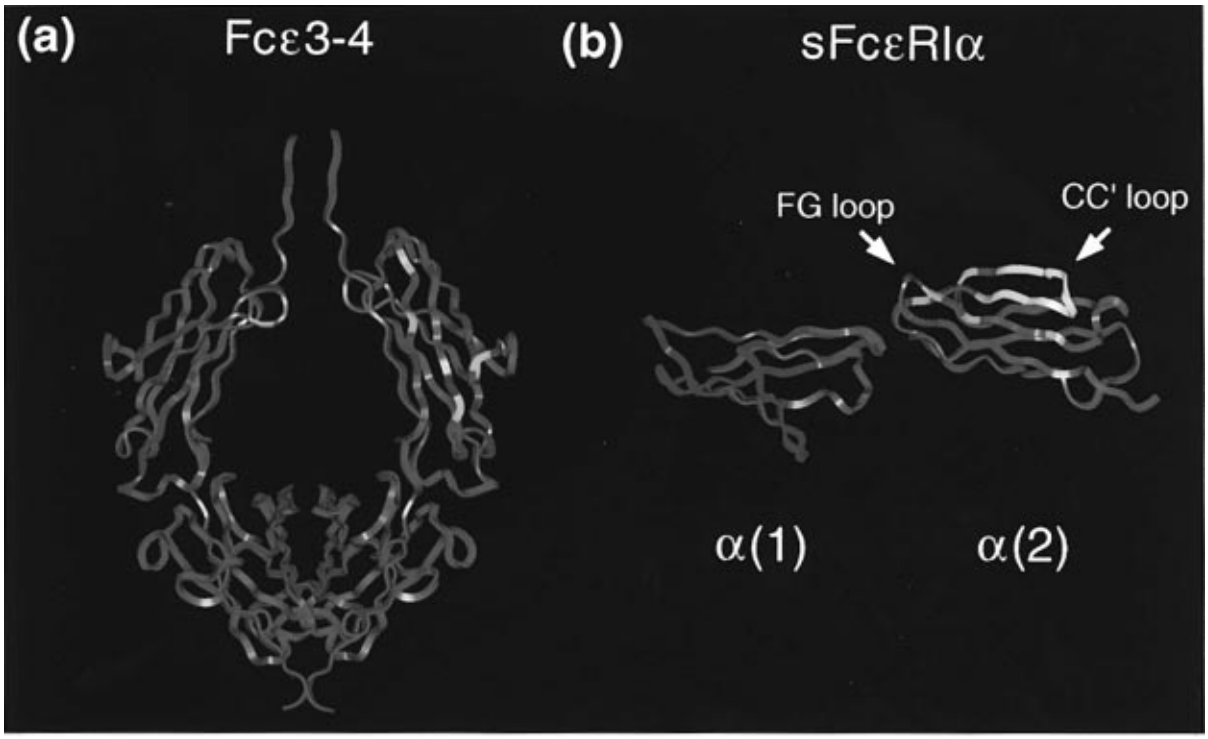

FIGURE 7: Location of contact residues in the modeled three-dimensional structures of IgE-Fc and sFcεRIα. (a) Fcε3-4 (after Helm et al., 1991). Residues demonstrated to be important in binding FcεRIα are colored orange (Presta et al., 1994) and red (Henry et al., 1997), and those shown not to be involved in these studies are colored in green. All the mutations are shown only on the front face of Fcε3-4. (b) FcεRIα domains 1 and 2 (after McDonnell et al., 1996; note that the relative disposition of the two domains is not defined). Sequences in α(1) demonstrated by homologue scanning mutagenesis to be uninvolved in the interaction with IgE are shown in green (Mallamaci et al., 1993). Residues in α(2) shown to be important for IgE binding are shown in yellow (McDonnell et al., 1996), orange (Danho et al., 1995) and red (this study).

studies with mutants of both sFcεRIα and IgE will be required to determine which of the two Cε3 domains in IgE contact the α(1) and α(2) domains in FcεRI.

Finally, the observation that the mutation D159K enhances the binding of sFcεRIα to IgE encourages us to believe that it may be possible to improve the affinity of smaller peptides derived from the receptor [cf. McDonnell et al. (1996)], so that they can effectively compete with the cell-bound receptor for IgE and be used in therapy.

ACKNOWLEDGMENT

We would like to thank P. M. Hogarth for the gift of the 3B4 anti-FcεRIα mAb, J.-P. Kinet for 15.1 anti-FcεRIα mAb, D. Stanworth for IgE-WT myeloma protein, and A. J. Beavil for additional purification of IgE-WT.

REFERENCES

Basu, M., Hakimi, J., Dharm, E., Kondas, J. A., Tsien, W. H., Pilson, R. S., Lin, P., Gilfillan, A., Haring, P., Braswell, E. H., Nettleton, M. Y., & Kochan, J. P. (1993) *J. Biol. Chem. 269*, 13118−13127.

Beavil, A. J., Beavil, R. L., Chan, C. M. W., Cook, J. P. D., Gould, H. J., Henry, A. J., Owens, R. J., Shi, J., Sutton, B. J., & Young, R. J. (1993) *Biochem. Soc. Trans. 21*, 968−972.

Bebbington, C. R., Renner, G., Thomson, S., King, D., Abrams, D., & Yarranton, G.T. (1992) *Biotechnology 10*, 169−175.

Bieber, T., de la Salle, H., Wollenberg, A., Hakimi, J., Chizzonite, R., Ring, J., Hanau, D., & de la Salle, C. (1992) *J. Exp. Med. 175*, 1285−1290.

Blank, U., Ra, C., Miller, L., White, K., Metzger, H., & Kinet, J.-P. (1989) *Nature 337*, 187−189.

Blank, U., Ra, C., & Kinet, J.-P. (1991) *J. Biol. Chem. 266*, 2639−2646.

Burt, D. S., Hastings, G. Z., & Stanworth, D. R. (1986) *Mol. Immunol. 23*, 181−191.

Chomczynski, P., & Sacchi, M. (1987) *Anal. Biochem. 162*, 156−159.

Cook, J. P. D. (1996) Ph.D. Thesis, University of London, Senate House, Malet Street, London, WC1E 7HU.

Danho, W., Makofske, R., Swistok, J., Mallamaci, M., Nettleton, M., Madison, V., Greeley, D., Fry, D., & Kochan, J. (1995) *The 9th International Congress of Immunology*, San Fransisco, Abstr. 4018.

Edwards, P. R., Gill, A., Pollard-Knight, D. V., Hoare, M., Buckle, P. E., Lowe, P. A., & Leatherbarrow, R. J. (1995) *Anal. Biochem. 231*, 210−217.

Gounni, A. S, Lamkhioued, B., Ochiai, K., Tanaku, Y., Deleporte, E., Capron, A., Kinet, J.-P., & Capron, M. (1994) *Nature 367*, 183−186.

Hakimi, J., Seals, C., Kondas, J. A., Pettine, L., Danho, W., & Kochan, J. (1990) *J. Biol. Chem. 265*, 22079−22081.

Hayter, P. M., Curling, E. M. A., Gould, M. L., Baines, A. J., Jenkins, N., Strange, P. G., & Bull, A. T. (1993) *Biotechnol. Bioeng. 42*, 1077−1085.

Helm, B. A., Ling, Y., Teale, C., Padlan, E. A., & Bruggemann, M. (1991) *Eur. J. Immunol. 21*, 1543−1548.

Henry, A. J., Cook, J. P. D., McDonnell, J. M., Mackay, G. A., Shi, J., Sutton, B. J., & Gould, H. J. (1997) *Biochemistry, 36*, 15568−15578.

Ho, S. N., Hunt, H. D., Horton, R. M., Pullen, J. K., & Pease, L. R. (1989) *Gene 77*, 51−59.

Hogarth, P. M., Hulett, M. D., Ierino, F. L., Tate, B., Powell, M. S., & Brinkworth, R. I. (1992) *Immunol. Rev. 125*, 21−35.

Hulett, M. D., Witort, E., Brinkworth, R. I., McKenzie, I. F. C., & Hogarth, P. M. (1994) *J. Biol. Chem. 269*, 15287−15293.

Kahn, P. C. (1979) *Methods Enzymol. 61*, 335−378.

Keown, M. B., Ghirlando, R., Young, R. J., Beavil, A. J., Owens, R. J., Perkins, S. J., Sutton, B. J., & Gould, H. J. (1995) *Proc. Natl. Acad. Sci. U.S.A. 92*, 1841−1845.

Keown, M. B., Ghirlando, R., Mackay, G. A., Sutton, B. J., & Gould, H. J. (1997) *Eur. Biopys. J. 25*, 471−476.

Kulczycki, A., & Metzger, H. (1974) *J. Exp. Med. 140*, 1676−1695
Laemmli, U. K. (1970) *Nature 227*, 690−685.
Letourner, O., Sechi, S., Willette-Brown, J., Robertson, M. W., & Kinet, J.-P. (1995) *J. Biol. Chem. 270*, 8249−8256.
Mallamaci, M. A., Chizzonite, R., Griffin, M., Nettleton, M., Hakimi, J., Tsien, W.-H., & Kochan, J. P. (1993) *J. Biol. Chem. 268*, 22076−22083.
Maurer, D., Fiebiger, E., Reininger, B., Wolffwiniski, B., Jouvin, M.-H., Kilgus, O., Kinet, J.-P., & Stingl, G. (1994) *J. Exp. Med. 179*, 745−750.
Maurer, D., Ebner, C., Reininger, B., Fiebiger, E., Kraft, D., Kinet, J.-P., & Stingl, G. (1995) *J. Immunol. 154*, 6285−6290.
McDonnell, J. M., Beavil, A. J., Mackay, G. A., Jameson, B. A., Korngold, R., Gould, H. J., & Sutton, B. J. (1996) *Nat. Struct. Biol. 3*, 419−426.
Metzger, H. (1992) *Immunol. Rev. 125*, 37−48
Miller, K. L., Duchemin, A.-M., & Anderson, C. L. (1996) *J. Exp. Med. 183*, 2227−2233
Padlan, E. A., & Davies, D. R. (1986) *Mol. Immunol. 23*, 1063−1075.
Padlan, E. A., & Helm, B. A. (1992) *Receptor 2*, 129−144
Presta, L., Shields, R., O'Connell, L., Lahr, S., Porter, J., Gorman, C., & Jardieu, P. (1994) *J. Biol. Chem. 42*, 26368−26373.
Ravetch, J. V., & Kinet, J.-P. (1991) *Annu. Rev. Immunol. 9*, 457−492.
Riske, F., Hakimi, J., Mallamaci, M., Griffin, M., Pilson, B., Tobkes, N., Lin, P., Danho, W., Kochan, J., & Chizzonite, R. (1991) *J. Biol. Chem. 266*, 11245−11251.
Robertson, M. W. (1993) *J. Biol. Chem. 268*, 12736−12743.
Sanger, F., Nicklen, S., & Coulsen, A. (1977) *Proc. Natl. Acad. Sci. U.S.A. 74*, 5463−5467.
Scarselli, E., Esposito, G., & Traboni, C. (1993) *FEBS Lett. 329*, 223−226.
Sechi, S., Roller, P. P., Willette-Brown, J., & Kinet, J.-P. (1996) *J. Biol. Chem. 271*, 19256−19263.
Shi, J., Ghirlando, R., Beavil, R. L., Beavil, A. J., Keown, M. B., Young, R. J., Owens, R. J., Sutton, B. J., & Gould, H. J. (1997) *Biochemistry 36*, 2112−2122.
Sutton, B. J., & Gould, H. J. (1993) *Nature 366*, 421−428.
Wang, B., Rieger, A., Kilgus, O., Ochiai, K., Maurer, D., Fodinger, D., Kinet, J.-P., & Stingl, G. (1992) *J. Exp. Med. 175*, 1353−1365.
Young, R. J., Owens, R. J., Mackay, G. A., Chan, C. M. W., Shi, J., Hide, M., Francis, D. M., Henry, A. J., Sutton, B. J., & Gould, H. J. (1995) *Protein Eng. 8*, 193−199.

BI9713005